The Eurasia Proceedings of Science, Technology, Engineering & Mathematics (EPSTEM)
ISSN: 2602-3199

The Eurasia Proceedings of Science, Technology, Engineering & Mathematics (EPSTEM), 2024

Volume 32, Pages 116-122

IConTES 2024: International Conference on Technology, Engineering and Science

Effects of Micro-Blowing and Vortex Generators on the Boundary Layer Separation Control of a NACA 0015 Airfoil

Mohammed Said Boutoudj
Mouloud Mammeri University of Tizi-Ouzou

Hocine Tebbiche
Mouloud Mammeri University of Tizi-Ouzou

Abstract: The flow on the upper surface of an airfoil is subject to an adverse pressure gradient when the incidence increases. This leads to boundary layer separation, causing losses in aerodynamic performance by decreasing lift and increasing drag. Various techniques, both passive and active, exist for boundary layer control to delay or eliminate fluid separation. Vortex generators (VGs) are simple use and among the most effective passive flow control solutions. They bring momentum from the external flow to the boundary layer, making it more resistant to separation. Active control methods, such as blowing through micro-holes, are also very effective but more challenging to implement. In the present work, a comparative experimental study of the flow control around a NACA 0015 airfoil is conducted in a subsonic wind tunnel using the two types of control strategies. The used VGs are the Lin's counter –rotating configuration. They are triangular shape, placed on the suction face at 10% of the airfoil chord. The active control solution proposed relates to a steady blowing carried out with an angle of 45° relative to chord line, through a series of micro-holes of 0.6 mm in diameter uniformly arranged also at 10% from the leading edge. An improvement in aerodynamic performance was achieved with both strategies, with a more significant increase of approximately 49% in lift and a reduction of about 69% in drag in the case of micro-blowing.

Keywords: NACA 0015 airfoil, Boundary layer, Vortex generators, Micro-blowing, Lift, Drag

Introduction

The flow on the upper surface airfoil is subject to an adverse pressure gradient when the incidence increases. This leads to the boundary layer separation which causes looses in the aerodynamic performances (lift decrease and drag increase). It is well known that the lift around an airfoil is rather created by the suction on the upper surface than the overpressure on the lower one. The flow control aims to delay or eliminate the fluid separation and its undesirable effects like vibrations and aerodynamic noise.

In the aircraft industries the flow control takes on capital importance for the reduction of the energy overconsumption and the aerodynamic noise. Moreover, during take-off or landing, the speed is low and the attack angle needs to be high for the lift enhancement. This situation is also encountered in wind turbine blades where the increase in the captured energy requires an increase in the incidence of the blades, particularly in the vicinity of the hub.

There are two types of boundary layer control (Gad-el-Hak, 2001). Active methods and passive ones. Active techniques require adding external energy to the boundary layer to make it more resistant to the separation. Methods such as suction, blowing (Huang et al., 2004). Or moving surfaces (Modi, 1997). Have been investigated in various applications. Active methods are however difficult to implement and they cause problems of congestion.

- This is an Open Access article distributed under the terms of the Creative Commons Attribution-Noncommercial 4.0 Unported License, permitting all non-commercial use, distribution, and reproduction in any medium, provided the original work is properly cited.

- Selection and peer-review under responsibility of the Organizing Committee of the Conference

© 2024 Published by ISRES Publishing: www.isres.org

Unlike active techniques, passive methods do not require any external energy supply. They are therefore easier to use but still have appreciable effectiveness. Among existing passive techniques, vortex generators (VGs) have proven to be very effective in controlling the flow separation. VGs were first introduced by Taylor (1947). And have been since widely investigated in several configurations. They are placed on a surface subject to an adverse gradient pressure and can be rectangular, triangular or aero shaped form. VGs produce streamwise vortices which induce momentum transfer from the freestream to the region close to the wall, leading to the delay or suppression of the boundary layer separation. Vortex generators enhance the aerodynamic performances and the most efficiency are the Lin's ones V-shaped when their height is less than the boundary layer thickness (Rao et al., 1988).

The main use of the VG is in the field of military or civil aviation, and recently in wind turbines with the objective of increasing lift and decreasing drag. Enhancement of the airfoil aerodynamic performances by VGs constitute a preliminary solution to passive control over a wind blade, even the flow in the last case is more complex because of the rotation. Wind blades equipped with VGs on the suction surface could be a potential solution to improve aerodynamic efficiency of horizontal axis wind turbines by delaying stall, increasing lift and reducing drag. The influence of the VGs geometrical parameters such as height, inclination angle or even their location on their aerodynamic performance has been reported by several authors (Lin, 2002; Godard et al., 2006; Fouatih et al., 2016; Bouderbala, 2025).

The present work focuses on the control flow around a NACA 0015 airfoil by means of two strategies: passive method by VGs and active technique by blowing. Experimental measurements of the aerodynamics forces (lift and drag) as well as the wall pressure field around the airfoil were undertaken. The effectiveness of each strategy is then examined.

Descrition of the Experiments

Wind Tunnel and Measuring Equipments

The experiments were conducted in a Deltalab™ type wind tunnel. The maximum measurable velocity exceeds 40 m/s. The turbulence level is set by a grid at the inlet with a size of 5×5 mm^2. The test section length and cross-sectional area are 100 cm and 30×30 cm^2, respectively. Lift and drag forces were measured using an aerodynamic balance connected to a data acquisition system. Each conducted test was repeated three times, and the average was considered. The acquisition time was set to 60 s with a frequency of 500 Hz. The pressure was given by a manometer which allows simultanous measurement until 24 pressure taps. The freestream velocity was measured using a Pitot tube connected to a differential oil pressure gauge (Tebbiche et al., 2019).

The blowing system consists of an air compressor, a stilling chamber, and a flow control valve. The Schneider-type compressor compresses air, achieving a maximum relative pressure of 16 bar. Compressed air flows through a valve used to regulate pressure in the generating state, then it is directed into the stilling chamber designed to minimize turbulence caused by the compressor. It is then conveyed to a ramp constructed from a copper tube with a diameter D=14mm, onto which capillary tubes are implanted, each having an outlet section with a diameter d=0.6mm. The capillary tubes are connected to the blowing orifices of the airfoil. More details about the blowing installation are given in a previous work (Tebbiche et al., 2021).

Passive Vortex Generators

Passive control by VGs is a strategy that does not require any external energy to the flow. Their particularity is to bring the momentum from the external flow to the near-wall flow regions. VGs can be co-rotating or counter-rotating. The second category is known to be more efficient because it generates better mixing between the external flow and the boundary layer (Lin, 2002).

In the case of an aerodynamic profile, the implantation of VGs line on its upper face leads to delay or even eliminate the detachment. Vortex generators are placed upstream of the baseline separation and their geometrical parameters such as the height h, the spacing λ, the relative incidence angle β as well as their position according to the chord length affect the flow control efficiency. Among these parameters, the height and the relative incidence angle particcularly are linked to the circulation of the generated vorticies.

Initially, Taylor in its experimental investigation, using triangular Vortex Generators, evaluated the height to the boundary-layer thickness δ (Taylor, 1947). Rao et al. (1988) tested different VGs configurations; the idea was to reduce the height by submerging them in the boundary layer. They estimated that h reduced to about 0.6δ is more effective compared to the classical one. Lin (1999) tested two different micro-generators configurations co-rotating and counter-rotating. His conclusion was that the VGs taken on counter-rotating mode at the threshold height $h/\delta \approx 0.2$ allows a significant improvement in control. For $h/\delta > 0.2$, an increase in drag is considered not as significantly improving their performances. For values of $h/\delta < 0.2$, a consistent decrease in the VGs efficiency is thus remarked. As for the optimal incidence angle, several works tend to evaluate it between 10 and 20 degrees (Fouatih et al., 2016).

In this work, the studied vortex generators are counter rotating, triangular shape and placed normal to the surface at 10% of the airfoil chord. They were manufactured using a very thin sheet metal of 0.3mm glued on plastic ribbons which facilitates their positioning in the precise location along the chord-wise and spanwise of the airfoil. The dimensions of the triangular plates are given in the Table 1. The line VGs was constituted by six generators.

The considered profile is the NACA 0015; the chord c length is 150 *mm* and the depth is equal to 200 *mm*. The airfoil is equipped with guard plates to eliminate edge effects and 14 pressure taps on the suction face for the measurement of the pressure fields. The boundary layer thickness estimated at 0.19c using a 2D-RANS numerical approach is about 10 mm for a Reynolds number Re = $2.5\ 10^5$ when the attack angle equals 13° (Tebbiche et al., 2019). Figure 1 shows the VGs and the airfoil.

Table 1. Geometrical characteristic of the tested VGs

H (mm)	*l (mm)*	*a* (mm)	λ (mm)	β (°)
5.5	14.3	7	13.5	15

H: height, *l*: length, *a*: space between the same VG, λ: distance between two passive devices, β: the relative incidence angle.

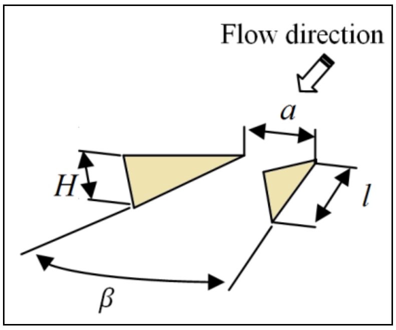

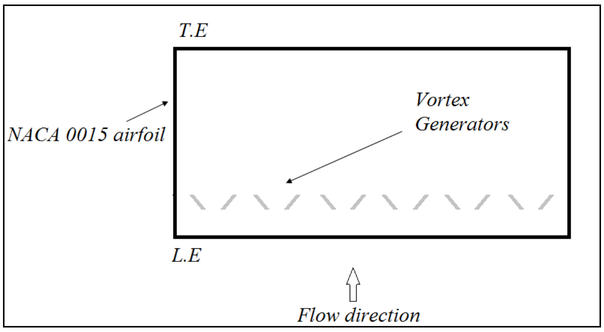

a) b)

Figure 1. a) Vortex generators. b) The line of VGs on the airfoil.

Active Control by Blowing

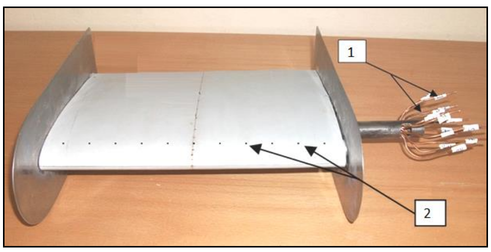

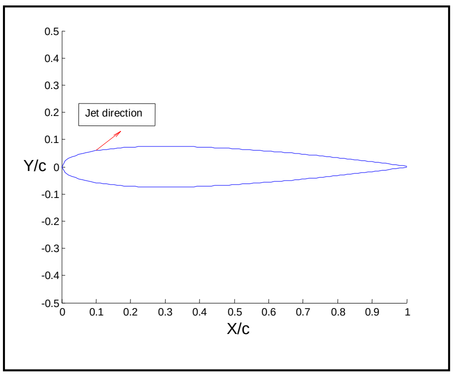

a) b)

Figure 2. a) Position of the blowing holes on the NACA 0015 airfoil. 1: Capillary air tubes, 2: Bowing Micro-holes, b) Jet direction

The active control strategy employed in this study is continuous blowing through micro-jets. Micro-holes with a diameter of 0.6 mm are linearly arranged on the wing upper surface at 10% from the leading edge. Unlike conventional control strategies, blowing through the micro-jets allows for a much deeper penetration of the jet into the flow and results in air consumption savings. The airfoil used in this case is identical to that described previously and used for the passive control. It is a NACA 0015 with a chord c = 150 *mm* and a depth equal to 200 *mm.* It is equipped with 10 micro-holes of 0.6 mm diameter evenly arranged at 10% of the leading edge. The micro-holes, employed for blowing, are oriented at a 45° angle relative to the wing's chord (Figure 2).

The blowing configuration can be likened to a convergent nozzle, where the nozzle throat corresponds to the cylindrical opening of the capillary tubes used for blowing. To better characterize the flow at the blowing orifices, it is essential to establish a relationship between the air pressures measured in the generating state and in the immediate vicinity of the micro-orifices, and the ejected air flow. The latter is determined by the following equation:

$$Q_j = S_j \sqrt{\frac{2k}{(k-1)} \frac{P_t}{\nu_t} \left(\left(\frac{P}{P_t} \right)^{2/k} - \left(\frac{P}{P_t} \right)^{(k+1)/k} \right)} \tag{1}$$

With: *k*: Adiabatic constant (*k = 1.2*), P_t: Total pressure in the generating state, : *P*: Static pressure at the outlet of the orifice, ν_t : Specific volume at the generating state. The jet velocity V_j is determined from the flow rate using the following expression:

$$V_j = \frac{\nu Q_j}{S_j} \tag{2}$$

Aerodynamic Coefficients

The interaction between the fluid and an airfoil results in two forces, lift and drag, which are commonly given by the two respective aerodynamic coefficients:

$$C_L = \frac{F_y}{\frac{1}{2} \rho U_\infty^2 S} \tag{1}$$

and

$$C_d = \frac{F_x}{\frac{1}{2} \rho U_\infty^2 S} \tag{2}$$

F_y and F_x are respectively the lift and the drag, ρ is the volumic weight, S the surface airfoil and U_∞ the upstream velocity.

Results and Discussion

Uncontrolled Flow around NACA 0015 Airfoil

Pressure Coefficient Distribution

Figure 3 presents a typical example of the upper surface pressure distribution for a Reynolds number of 2.5×10^5. At low angles of attack, no clear evidence of a bubble is shown by the pressure distribution. When the incidence reaches 11 degrees, a bubble that is approximately 11% of the chord length appears very close to the leading edge. Between 11° and 15°, the bubble length decreases to about 7%. As the angle of attack increases, the pressure difference between the upper and lower surfaces also increases until leading edge laminar separation occurs, as shown at an angle of attack of 16°. Here, the measured pressure at the separation point is almost the same for all pressure taps along the profile. This is clearly evident through the appearance of a plateau in the upper surface pressure data.

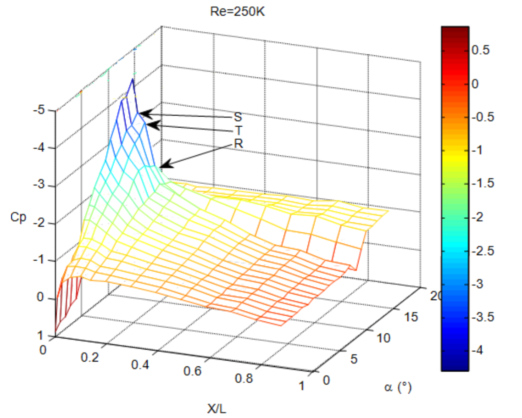

Figure 3. Cp coefficient vs X/L at various attack angles. **S**: Laminar separation, **T**: Transition, **R**: Reattachment.

Lift and Drag Coefficient Curves

The characteristics of the lift and drag coefficients for Reynolds numbers from 1.5×10^5 to 3×10^5 are presented in Figure 4. These curves are used as reference; the given results are not corrected as the main objective being the contribution of the control on the aerodynamic coefficients. The uncontrolled flow is characterized by a stall which occurs for an incidence around α= 15°. The sudden drop in lift is accompanied by a high production of the drag.

An increase in the maximum lift coefficient is observed as the Reynolds number increased. A variation in Reynolds number affects the slope of the lift curve, which is influenced by flow separation on the upper surface of the airfoil. It is well known that a decrease in Reynolds number extends the length of laminar separation bubbles on the upper surface and leads to complete flow separation at low angles of attack. Non-linear behavior is observed for the different Reynolds numbers tested. This non-linearity is related to the presence of flow separations on the upper surface of the airfoil at different angles of attack.

The non-linear phenomenon in the lift curve slope can be explained by two distinct phenomena that occur in low Reynolds number flows ($10^5 < Re < 10^6$). Between 0 and 8 degrees angle of attack, there is a separation bubble on the upper surface of the airfoil that moves from the trailing edge toward the leading edge, altering the transition point of the flow from laminar to turbulent. After approximately 8 degrees, a conventional separation bubble near the trailing edge forms as the angle of attack increases, eventually leading to complete separation on the upper surface of the airfoil, known as stall. Drag also increases at lower angles of attack as the Reynolds number raises, indicating an earlier onset of flow separation. After stall, the drag coefficient increases significantly as shown in figure 4b.

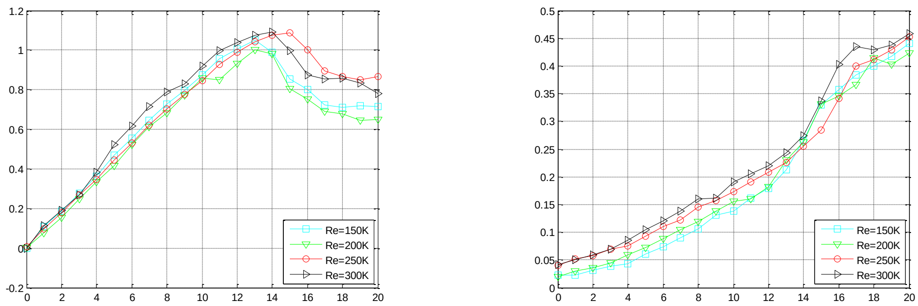

a) b)

Figure 4. Lift and drag coefficients versus angles of attack at various Reynolds numbers.
a) Lift coefficient, b) Drag coefficient

Controlled Flow

Passive Flow Control Using VGs

Figure 5 shows the C_L and C_d evolutions versus the incidence angle for both the reference case and the controlled flow. One can see in Figure 4a a delay in stall of two degrees and a lift enhancement between 14° and 17°. Figure 4b shows a decrease in drag from α= 10° which becomes more pronounced post stall. These variations result in an improvement of 52% for the ratio C_L/C_D .

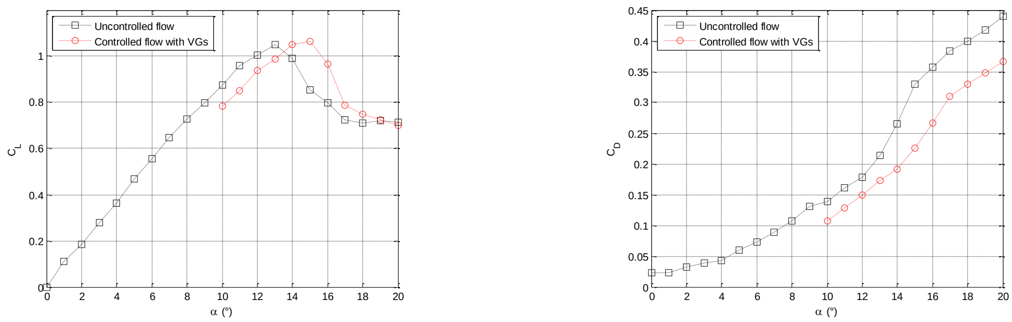

a) b)

Figure 5. Lift and drag coefficients versus angles of attack. With and without control using VGs, Re=1.5×10^5. a) Lift coefficient, b) Drag coefficient

Controlled Flow with Micro-Blowing

Figure 6 shows the C_L and C_D evolutions versus the incidence angle for both the reference case and the controlled flow by blowing. Three mass flow rates were considered: 0.75 g/s, 0.91 g/s and 1.06 g/s. Figure 6a shows a significant increase in the lift coefficient and a delay in stall of four degrees when the flow is controlled. The lift increase is linked to the blowing flow rate. Figure 6b shows a decrease in drag for the entire range of the incidences, from α= 0° to α= 20°. Furthermore, one can see an important gap between the reference case and the controlled flow when the incidence exceeds 12°. An improvement in aerodynamic performance was achieved with an increase of approximately 49% in lift, a reduction of about 69% in drag and an enhancement of 75% for the ratio C_L/C_D .

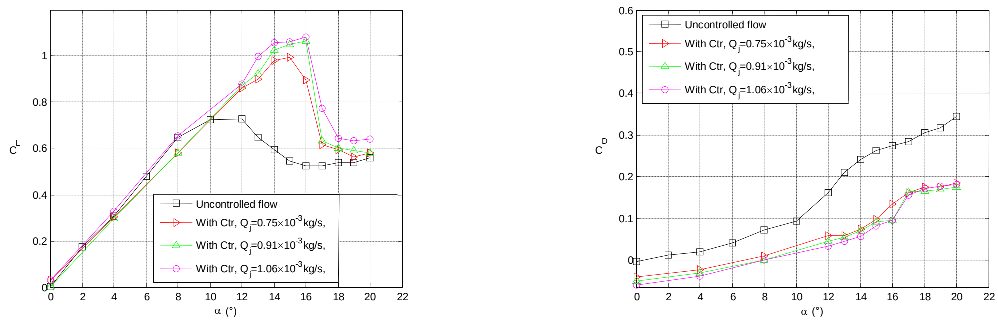

a) b)

Figure 6. Lift and drag coefficients versus angles of attack. With and without control using micro-blowing, Re=1.5×10^5, a) Lift coefficient, b) Drag coefficient.

Conclusion

This study presents a comparative analysis of flow control around a NACA 0015 airfoil conducted in a subsonic wind tunnel, utilizing both passive and active control strategies. The passive control strategy employed Lin's counter-rotating vortex generators (VGs) of triangular shape, positioned normal to the upper surface at 10% of the airfoil chord. The results demonstrated a delay in stall by two degrees and an improvement of 52% in the lift-to-drag ratio (C_L/C_D). The active control solution proposed relates to a steady blowing carried out with an angle of 45° relative to chord line, through a series of micro-holes of 0.6 mm in diameter uniformly arranged also at 10% from the leading edge. This approach yielded an even more significant delay in stall of four degrees and a substantial improvement of 75% in the C_L/C_D ratio, underscoring the effectiveness of active control methods. Overall, the findings indicate that both strategies enhance aerodynamic performance, each with distinct advantages and disadvantages. The passive control method using Lin's counter-rotating vortex generators (VGs) is straightforward and requires minimal maintenance, though its effectiveness is limited. In contrast, the active control method with steady blowing through micro-holes offers superior enhancements, such as greater stall delay and improved lift-to-drag ratio, but comes with increased complexity and energy consumption. Thus, while the active method provides significant benefits, the passive method serves as a more accessible alternative, highlighting the importance of context in selecting a flow control strategy.

Scientific Ethics Declaration

The authors declare that the scientific ethical and legal responsibility of this article published in EPSTEM Journal belongs to the authors

Acknowledgements or Notes

This article was presented as a poster presentation at the International Conference on Technology, Engineering and Science (www.icontes.net) held in Antalya/Turkey on November 14-17, 2024.

References

Bouderbala, F. (2025). Passive flow control around a NACA4415 airfoil by means of vortex generators. *International Journal of Fluid Mechanics Research*, *52*(1), 1-16.

Fouatih, O. M., Medale, M., Imine, O., & Imine, B. (2016). Design optimization of the aerodynamic passive flow control on NACA 4415 airfoil using vortex generators. *European Journal of Mechanics-B/Fluids*, *56*, 82-96.

Gad-el-Hak, M. (2001). Flow control: The future. *Journal of Aircraft*, *38*(3), 402–418.

Godard, G., & Stanislas, M. (2006). Control of a decelerating boundary layer. Part 1: Optimization of passive vortex generators. *Aerospace Science and Technology*, *10*(3), 181-191.

Huang, L., Huang, P. G., LeBeau, R. P., & Hauser, T. (2004). Numerical study of blowing and suction control mechanism on NACA0012 airfoil. *Journal of Aircraft*, *41*(5), 1005-1013.

Lin, J. C. (2002). Review of research on low-profile vortex generators to control boundary-layer separation. *Progress in Aerospace Sciences*, *38*(4-5), 389-420.

Lin, J. C. (1999). Control of turbulent boundary-layer separation using micro-vortex generators. *30th Fluid Dynamics Conference*, 3404.

Modi, V. J. (1997). Moving surface boundary-layer control, a review. *Journal of Fluids and Structures*, *11*(6), 627-663.

Rao, D., & Kariya, T. (1988). Boundary-layer submerged vortex generators for separation control-an exploratory study. *1st National Fluid Dynamics Conference*, 3546.

Taylor, H. D. (1947). The elimination of diffuser separation by vortex generators. *United Aircraft Corporation Research Department* ,103.

Tebbiche, H., & Boutoudj, M. S. (2021). Active flow control by micro-blowing and effects on aerodynamic performances. Ahmed body and NACA 0015 airfoil. *International Journal of Fluid Mechanics Research*, *48*(2).

Tebbiche, H., & Boutoudj, M. S. (2019). Turbulent flow control with vortex generators around a symmetrical airfoil at high attack angles. *Journal of the Serbian Society for Computational Mechanics*, *13*(2), 67-85.

Author Information

Mohammed Saîd Boutoudj	**Hocine Tebbiche**
Laboratoire d'Energétique, Mécanique et Matériaux – LEMM, Mouloud MAMMERI University of Tizi-Ouzou 15000, Tizi-Ouzou, Algeria Contact e-mail: *mohammedsaid.boutoudj@ummto.dz*	Laboratoire d'Energétique, Mécanique et Matériaux – LEMM Mouloud MAMMERI University of Tizi-Ouzou 15000, Tizi-Ouzou, Algeria

To cite this article:

Boutoudj, M.S. & Tebbiche, H. (2024). Effects of micro-blowing and vortex generators on the boundary layer separation control of a NACA 0015 airfoil. *The Eurasia Proceedings of Science, Technology, Engineering & Mathematics (EPSTEM), 32*, 116-122.